Effective radiative properties of bounded cascade absorbing clouds: Definition of an effective single-scattering albedo

Frédéric Szczap, Harumi Isaka, Marcel Saute, Bernard Guillemet, Andrey Ioltukhovski

JOURNAL OF GEOPHYSICAL RESEARCH, VOL. 105, NO. D16, PAGES 20,635–20,648, AUGUST 27, 2000

Effective radiative properties of bounded cascade absorbing clouds: Definition of an effective single-scattering albedo

Frédéric Szczap, Harumi Isaka, Marcel Saute, and Bernard Guillemet

Laboratoire de Météorologie Physique, Université Blaise Pascal, Aubière, France

Andrey Ioltukhovski

Keldish Institute of Applied Mathematics, Moscow

Abstract. We applied the equivalent homogeneous cloud approximation (EHCA) to the bounded cascade inhomogeneous absorbing clouds and defined their effective radiative properties. It is found that we have to introduce an effective single-scattering albedo in addition to an effective optical depth to treat the inhomogeneous absorbing clouds under the plane-parallel homogeneous cloud assumption. For an inhomogeneous absorbing cloud, a pair of the effective parameters can be estimated from each one of three possible pairs taken from the area-averaged reflectance, transmittance and absorptance. We found that the behavior of these effective properties was quite similar to those observed for the inhomogeneous non absorbing clouds except that two effective parameters were to be examined instead of only one effective parameter for the nonabsorbing clouds. Empirical relations for both the effective optical depth and the single-scattering albedo were given as a function of the local mean optical depth and relative local cloud inhomogeneity. We showed that the effective single-scattering albedo could not be properly introduced under the effective thickness approximation (ETA), which indicates an important conceptual difference between the EHCA and the ETA. Finally, we discussed possible consequences of the effective single-scattering albedo, defined in this study, with respect to the anomalous absorption phenomenon.

1. Introduction

In the companion paper [*Szczap et al.*, this issue] (hereinafter referred to as SZ1), we proposed the equivalent homogeneous cloud approximation (EHCA) and studied the effect of cloud inhomogeneity on the effective radiative properties of the bounded cascade nonabsorbing clouds. Natural clouds absorb a part of incoming solar radiation, and their absorption efficiency varies with the wavelength and size distribution of cloud particles, and also with the nature and concentration of aerosol particles and other pollutants. *Borde and Isaka* [1996] suggested that a multifractal absorbing cloud might be treated as a plane-parallel homogeneous cloud, by using its effective optical depth and keeping its single-scattering albedo unchanged. However, this approximation led to a small but finite systematic bias in the absorptance. On the other hand, *Cairns et al.* [2000] recently showed that cloud inhomogeneity affected cloud absorption efficiency at GCM scale and that this effect varied with the mean optical depth of the inhomogeneous clouds. *Titov* [1998] also investigated the contributions of "subpixel scale" cloud inhomogeneity and horizontal photon transport on the absorption of inhomogeneous clouds. This raises a question of how absorption modifies the effect of the cloud inhomogeneity on the effective radiative properties of the inhomogeneous clouds under EHCA.

The retrieval of cloud parameters from multispectral radiometric data is another field of interest in which we need to specify the effect of cloud inhomogeneity, especially the effect on the single-scattering albedo. The knowledge of such an effect is important, because the retrieval of effective radius relies on the droplet size dependency of the single scattering albedo in near infrared [*Nakajima and King,* 1988, 1990; *Twomey and Cocks,* 1989; *Wetzel and Vonder Haar,* 1991]. Estimating and correcting the cloud-inhomogeneity effect on the retrieved cloud parameters are relevant to moderate-resolution radiometric data provided by advanced very high resolution radiometer (AVHRR), Moderate Imaging Spectro-radiometer (MODIS) and Global Imager

Paper number 2000JD900145.
0148-0227/00/2000JD900145$09.00

(GLI) on ADEOS 2. This requires precise knowledge of relationships between the retrieved cloud parameters and the cloud inhomogeneity at subpixel scale, as already discussed by SZ1.

In this paper we extend the EHCA to inhomogeneous absorbing clouds and define their effective radiative properties under the EHCA. It is found that treating an inhomogeneous absorbing cloud as a plane-parallel homogeneous cloud requires the definition of an effective single-scattering albedo in addition to the effective optical depth. This finding is highly relevant to the retrieval of effective radius, because this retrieval is based, as noted above, on the droplet size dependency of the single-scattering albedo in near infrared. Furthermore, we investigate how these effective parameters vary with the solar incidence angle and scale of averaging. Empirical relations for both the effective optical depth and the effective-single scattering albedo are proposed as a function of optical and structural properties of inhomogeneous clouds.

Cahalan et al. [1994a,b] proposed the equivalent thickness approximation (ETA), which is based on the independent pixel approximation (IPA). However, there is a significant conceptual difference between the EHCA and the ETA as already discussed by SZ1. In this study we try to clarify the difference by analyzing the possibility of defining the effective single-scattering albedo under the ETA. Finally, we discuss the anomalous absorption phenomenon from the point of view of the EHCA.

2. Conditions of Simulation

The conditions of Monte Carlo (MC) simulation are practically the same as in the work of SZ1. We use the same MC code [*Marshak et al.,* 1995] except that we have modified it to estimate the photon absorption in each cloud pixel. Inhomogeneous clouds are generated with the bounded cascade model with eight cascades. The cloud domain is 12.8 km wide and 0.3 km thick, and it is composed of 256 vertically uniform "bar" clouds 50 m wide. The lateral boundary conditions are cyclic to form a cloud layer with infinite horizontal extent. We again use C1 cloud droplet distribution [*Garcia and Siewert,* 1985], and its volume-scattering phase function, computed for the nonabsorbing clouds, to the absorbing clouds for the reason of simplification. We assume a constant single-scattering albedo 0.97 for bounded cascade clouds, while we vary it between 0.9 and 1 for homogeneous clouds. In this study we often qualify the single-scattering albedo as "nominal" to emphasize the fact that it is only a "prescribed constant" and not "area-average" value independent of the droplet size distribution. As for the asymmetry factor, we implicitly keep it constant because we use the volume-scattering phase function computed for C1 droplet size distribution; changing its value would not be consistent with the use of C1 volume scattering phase function. On the other hand, *Borde and Isaka* [1996] already studied the effect of the asymmetry factor on the effective optical depth. Its variation would be small enough and could be neglected for droplet size distributions in shallow low-level stratiform clouds [*Davies et al,* 1984].

The transmittance decreases very rapidly with the increase in the optical depth because of the absorption. Hence MC simulation of the bounded cascade clouds is limited to a range of "cloud-mean optical depth" from 0.5 to 40 and three incidence angles (0°, 30°, and 60°). We sometimes qualify a mean optical depth as "cloud-mean" to stress that averaging is taken over the entire cloud domain (12.8 km) and not over a cloud segment ($L < 12.8$ km) . As in SZ1, three bounded cascade clouds were generated independently for each value of cloud-mean optical depths except for a special series of simulations. As for the number of photons, we almost doubled it from 3×10^7 of SZ1 to 5×10^7 photons to keep the MC relative intrinsic error to $\simeq 5 \times 10^{-3}$ as in SZ1. The area-averaged reflectance, transmittance, and absorptance of cloud segments were estimated again by randomizing their positions within the simulated clouds.

3. Analyses of Simulations

3.1. Definition of Effective Radiative Properties of an Inhomogeneous Absorbing Cloud

In SZ1 we defined the effective radiative properties of an inhomogeneous nonabsorbing cloud, by considering both reflectance and transmittance. However, when we deal with an inhomogeneous absorbing cloud, we have to consider the absorptance in addition to reflectance and transmittance to define its equivalent counterparts. This leads, as shown, to a significant difference in the definition of effective radiative properties between the nonabsorbing clouds and the absorbing clouds. It should be emphasized that we discuss here only the equivalence in the radiant flux and radiation budget and not the equivalence in the radiance field or bidirectional reflectance field.

If the volume-scattering phase function does not change too much with the droplet size distribution, we can characterize a plane-parallel homogeneous (PPH) absorbing cloud with two "independent" cloud parameters, i.e., the optical depth τ and single-scattering albedo ω . A PPH absorbing cloud is represented as a point $R_{\rm hom}, T_{\rm hom}, A_{\rm hom})$ on the $R+T+A=1$ plane in (R, T, A) space; R, T, and A designate, respectively, the reflectance, transmittance, and absorptance, i.e., three radiant flux components of the radiation budget.

We computed $(R_{\rm hom}, T_{\rm hom}, A_{\rm hom})$ for different pairs of the optical depth and single-scattering albedo and plotted them in (R, T, A) space. Figure 1 shows a grid composed of constant optical depth curves $\tau(R, T, A)$ and constant single-scattering curves $\omega(R, T, A)$ on the $R+T+A=1$ plane. It is for the 0° incidence angle; this

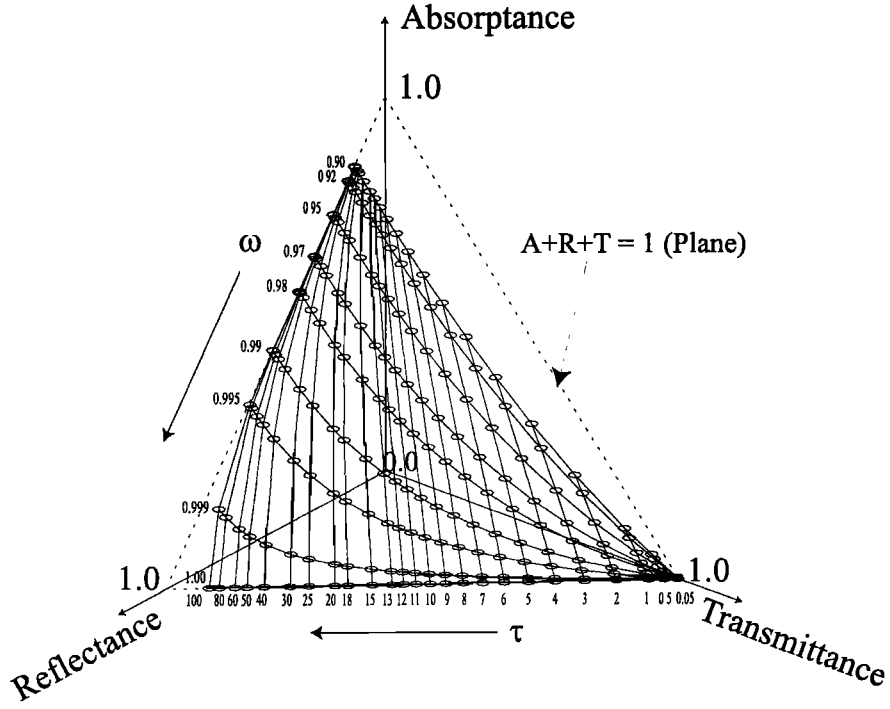

Figure 1. Schematic representation of the grid used for the determination of τ_{eff} and ω_{eff} for inhomogeneous clouds in (R, T, A) space. The grid is formed by the curves representing constant optical depth $\tau(R, T, A)$ and constant single-scattering curves $\omega(R, T, A)$ on the $R + T + A = 1$ plane.

τ, ω grid slightly changes with the solar incidence angle θ_0. These constant $\tau(R, T, A)$ and $\omega(R, T, A)$ curves are defined only on the $R + T + A = 1$ plane, and only two of R, T, and A are independent.

When the area-averaged reflectance, transmittance, and absorptance of an inhomogeneous absorbing cloud $(R_{\text{inhom}}, T_{\text{inhom}}, A_{\text{inhom}})$ are taken over the entire cloud domain, the point $(R_{\text{inhom}}, T_{\text{inhom}}, A_{\text{inhom}})$ is on the $R + T + A = 1$ plane because of the zero net horizontal photon transport between the cloud domain and its adjacent clouds. In this case we can always find an equivalent plane-parallel homogeneous cloud, whose radiant flux components are identical to $(R_{\text{inhom}}, T_{\text{inhom}}, A_{\text{inhom}})$ of the inhomogeneous cloud. The optical depth and single-scattering albedo of this equivalent PPH cloud can be read on the grid of Figure 1; they provide the effective optical depth and single-scattering albedo $(\tau_{\text{eff}}, \omega_{\text{eff}})$ of the inhomogeneous cloud in question.

Since only two of R, T, and A are independent, we can define only two effective radiative parameters even if more than two cloud parameters may be used to characterize inhomogeneous clouds. We use here the optical depth and single-scattering albedo to describe the cloud characteristics for the reason of commodity, but also because they are habitually used in the cloud radiation literature. However, they are not "intrinsic" cloud parameters from the microphysical point of view. It would be better, in principle, to characterize the clouds with appropriate independent microphysical parameters (effective radius, liquid water content, droplet number concentration) instead of radiative parameters (optical depth, single-scattering albedo, and asymmetry factor) which are correlated to each other.

We apply the same method as in SZ1 to analyze the deviations of the effective optical depth $\delta\tau_{\text{eff}} = \tau_{\text{eff}} - \bar{\tau}$ and effective single-scattering albedo $\delta\omega_{\text{eff}} = \omega_{\text{eff}} - \bar{\omega}$ from the homogeneous cloud point $(R_{\text{hom}}, T_{\text{hom}}, A_{\text{hom}})$ to the inhomogeneous cloud point $(R_{\text{inhom}}, T_{\text{inhom}}, A_{\text{inhom}})$. When R and T are chosen as independent variables of τ_{eff} and ω_{eff}, we can express these deviations as

$$\begin{aligned} \delta\tau_{\text{eff}} &= \frac{\partial\tau^{RT}}{\partial R}\delta R + \frac{\partial\tau^{RT}}{\partial T}\delta T \\ \delta\omega_{\text{eff}} &= \frac{\partial\omega^{RT}}{\partial R}\delta R + \frac{\partial\omega^{RT}}{\partial T}\delta T, \end{aligned} \tag{1}$$

where τ^{RT} and ω^{RT} represent the constant $\tau(R, T)$ and $\omega(R, T)$ curves on the $R+T+A = 1$ plane, and δR and δT are given, respectively, by $\delta R = R_{\text{inhom}} - R_{\text{hom}}$ and $\delta T = T_{\text{inhom}} - T_{\text{hom}}$. The above $\delta\omega_{\text{eff}}$ equation shows clearly that if $(\partial\omega^{RT}/\partial R)\delta R + (\partial\omega^{RT}/\partial T)\delta T \neq 0$, the single-scattering albedo cannot be maintained at its nominal value. Consequently, we have to introduce an effective single-scattering albedo in addition to the effective optical depth to define an equivalent homogeneous absorbing cloud. This finding implies that if we apply the PPH cloud assumption to an inhomogeneous absorbing cloud, we have to admit an apparent effect of cloud inhomogeneity on the absorption. This may explain a systematic bias we found in the radiant

flux of equivalent homogeneous clouds when the single-scattering albedo was kept unchanged [*Borde and Isaka*, 1996].

Figure 2 is the grid of Figure 1 projected onto the (R,T) plane. The point C represents a homogeneous cloud point with $\bar{\tau} = 10$ and $\bar{\omega} = 0.97$. The point C' represents the corresponding inhomogeneous cloud point with the same $\bar{\tau}$ and $\bar{\omega}$. The radiant flux was averaged over the entire cloud domain. The point C' ($\tau_{\text{eff}} = 6.89, \omega_{\text{eff}} = 0.964$) is located slightly off the $\omega(R,T) = 0.97$ curve, as suggested above by the $\delta\omega_{\text{eff}}$ equation. We can easily show that when $R_{\text{inhom}} + T_{\text{inhom}} + A_{\text{inhom}} = 1$ is satisfied, the effective single-scattering albedo is always smaller than the nominal single scattering albedo. For the cloud parameter retrieval, we use the effective radius as cloud parameter instead of the single-scattering albedo. In this case, the above finding implies that the cloud inhomogeneity has an apparent effect on the effective radius retrieved under the PPH cloud assumption, and an inhomogeneous absorbing cloud behaves as if it has an effective radius larger than the nominal effective radius.

When averaging is done over an area smaller than the entire cloud domain, the net horizontal photon transport between the cloud segment and the adjacent cloud cells may not be neglected: $R'_{\text{inhom}} + T'_{\text{inhom}} + A'_{\text{inhom}} = 1 + \varepsilon$ with $\varepsilon \neq 0$. The effective optical depth and effective single scattering albedo of a cloud segment with a horizontal extent L are referred as "local effective optical depth" [$\tau_{\text{eff}}(L)$] and "local effective single-scattering albedo" [$\omega_{\text{eff}}(L)$] as in SZ1. We can describe how the ε term affects these effective parameters, by applying the same analysis as in SZ1.

The difference between $(R'_{\text{inhom}}, T'_{\text{inhom}}, A'_{\text{inhom}})$ and $(R_{\text{hom}}, T_{\text{hom}}, A_{\text{hom}})$, both with the same $\bar{\tau}(L)$ and $\bar{\omega}(L)$, can be represented as a sum of two displacements in (R,T,A) space. The notations $\bar{\tau}(L)$ and $\bar{\omega}(L)$ indicate that these averages are defined over a cloud segment of L , but we omit (L) to abridge the notations if there is no risk of confusion. The first displacement is from the homogeneous cloud point $(R_{\text{hom}}, T_{\text{hom}}, A_{\text{hom}})$ to an intersection point $(R_{\text{int}}, T_{\text{int}}, A_{\text{int}})$ defined by the normal from $(R'_{\text{inhom}}, T'_{\text{inhom}}, A'_{\text{inhom}})$ to the $R + T + A = 1$ plane. This displacement occurs because the vec-

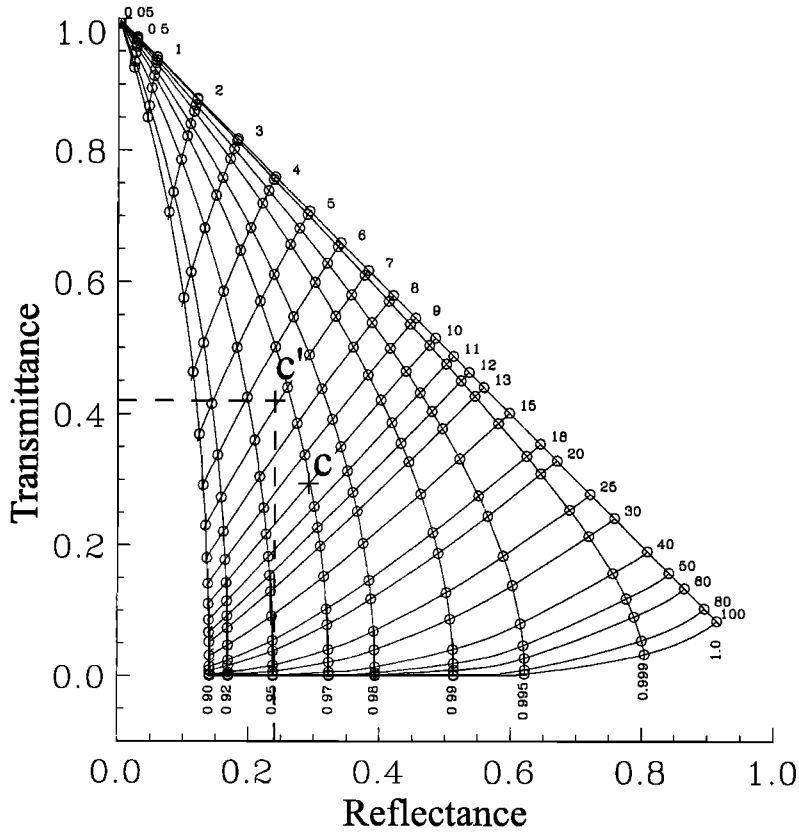

Figure 2. Grid composed of $\tau(R,T,A)$ and $\omega(R,T,A)$ curves projected on the (R,T) plane. The C point is the reflectance and transmittance of a homogeneous cloud having a mean optical depth 10 and single-scattering albedo 0.97. The C' point corresponds to an inhomogeneous cloud having the same mean optical depth and single-scattering albedo. It corresponds to a PPH cloud with $\tau_{\text{eff}} = 6.89$ and $\omega_{\text{eff}} = 0.964$.

tors $(R'_{\text{inhom}}, T'_{\text{inhom}}, A'_{\text{inhom}})$ and $(R_{\text{int}}, T_{\text{int}}, A_{\text{int}})$ are not directed to the same direction but also because of the ε term. It is expressed as

$$\begin{aligned}\delta\tau_{\text{int}} &= \frac{\partial\tau^{RT}}{\partial R}(R_{\text{int}} - R_{\text{hom}}) + \frac{\partial\tau^{RT}}{\partial T}(T_{\text{int}} - T_{\text{hom}}) \\ \delta\omega_{\text{int}} &= \frac{\partial\omega^{RT}}{\partial R}(R_{\text{int}} - R_{\text{hom}}) + \frac{\partial\omega^{RT}}{\partial R}(T_{\text{int}} - T_{\text{hom}}).\end{aligned} \tag{2}$$

The second displacement is from the intersection point $(R_{\text{int}}, T_{\text{int}}, A_{\text{int}})$ to the inhomogeneous cloud point $(R'_{\text{inhom}}, T'_{\text{inhom}}, A'_{\text{inhom}})$, which is due only to the ε term. We can estimate it only by projecting the grid of Figure 1 onto one of the (R,T), (T,A), and (A,R) planes. When the (R,T) plane is chosen as a projection plane, we are considering a displacement from $(R_{\text{int}}, T_{\text{int}}, A_{\text{int}})$ to $(R'_{\text{inhom}}, T'_{\text{inhom}}, A'_{\text{inhom}} - \varepsilon)$ on the $R+T+A=1$ plane. In this case, the deviations are expressed as

$$\begin{aligned}\delta\tau_{\varepsilon}(R,T) &= \left(\frac{\partial\tau^{RT}}{\partial R} + \frac{\partial\tau^{RT}}{\partial T}\right)\frac{\varepsilon}{3} \\ \delta\omega_{\varepsilon}(R,T) &= \left(\frac{\partial\omega^{RT}}{\partial R} + \frac{\partial\omega^{RT}}{\partial T}\right)\frac{\varepsilon}{3},\end{aligned} \tag{3}$$

where the partial derivatives are estimated at the intersection point. We obtain the similar expressions for $\delta\tau_{\varepsilon}(T,A)$ and $\delta\omega_{\varepsilon}(T,A)$ and for $\delta\tau_{\varepsilon}(A,R)$ and $\delta\omega_{\varepsilon}(A,R)$. These deviations have to satisfy

$$\begin{aligned}\delta\tau_{\varepsilon}(R,T) + \delta\tau_{\varepsilon}(T,A) + \delta\tau_{\varepsilon}(A,R) &= 0 \\ \delta\omega_{\varepsilon}(R,T) + \delta\omega_{\varepsilon}(T,A) + \delta\omega_{\varepsilon}(A,R) &= 0.\end{aligned} \tag{4}$$

3.2. Properties of τ_{eff} and ω_{eff}

3.2.1. Internal consistency of EHCA. When the ε term remains small to moderate, we can determine three pairs of $\tau_{\text{eff}}(L)$ and $\omega_{\text{eff}}(L)$: $[\tau^{RT}_{\text{eff}}(L), \omega^{RT}_{\text{eff}}(L)]$, $[\tau^{TA}_{\text{eff}}(L)$, $\omega^{TA}_{\text{eff}}(L)]$, and $[\tau^{AR}_{\text{eff}}(L)$, $\omega^{AR}_{\text{eff}}(L)]$ respectively; the superscripts RT , TA , and AR indicate the components of radiant flux used to retrieve $\tau_{\text{eff}}(L)$ and $\omega_{\text{eff}}(L)$. These three pairs correspond to the points $(R'_{\text{inhom}}, T'_{\text{inhom}}, A'_{\text{inhom}} - \varepsilon)$, $(R'_{\text{inhom}} - \varepsilon, T'_{\text{inhom}}, A'_{\text{inhom}})$, and $(R'_{\text{inhom}}, T'_{\text{inhom}} - \varepsilon, A'_{\text{inhom}})$ respectively. This is exactly the same situation as in SZ1 except that we are dealing now with three pairs of $\tau_{\text{eff}}(L)$ and $\omega_{\text{eff}}(L)$ instead of two estimates $\tau^{R}_{\text{eff}}(L)$ and $\tau^{T}_{\text{eff}}(L)$ in SZ1. When the ε term becomes too large, we cannot determine all the three possible pairs but only pairs for which the projected inhomogeneous cloud point is inside the projected grid.

We examine first $\tau_{\text{eff}}(L)$ and $\omega_{\text{eff}}(L)$ "retrieved" from the radiant flux components averaged over the entire cloud domain $L = 12.8$ km and for $\theta_0 = 0°$. Figure 3 a represents $\tau^{AR}_{\text{eff}}(L)$ and $\tau^{TA}_{\text{eff}}(L)$ as a function of $\tau^{RT}_{\text{eff}}(L)$ and Figure 3 b $\omega^{AR}_{\text{eff}}(L)$ and $\omega^{TA}_{\text{eff}}(L)$ as a function of $\omega^{RT}_{\text{eff}}(L)$. Three estimates are almost identical to each other because of the quasi-zero net horizontal photon transport at this averaging scale. The effective single-scattering albedo differs from its nominal value $\bar{\omega} = 0.97$ and varies from $\omega_{\text{eff}} = 0.965$ to 0.97. The variation of ω_{eff} is less than 0.5%, but it may still have a significant effect on the absorptance of the cloud as shown in section 5.

The effective optical depth and single-scattering albedo can also be estimated for cloud segments. Figures 4 a and 4 b are the same as Figures 3 a and 3 b, but for a horizontal scale of $L = 1.6$ km. The dispersion of $\tau_{\text{eff}}(L)$ is still small; it is slightly larger between $\tau^{AR}_{\text{eff}}(L)$ and $\tau^{RT}_{\text{eff}}(L)$ than between $\tau^{TA}_{\text{eff}}(L)$ and $\tau^{RT}_{\text{eff}}(L)$. Almost all

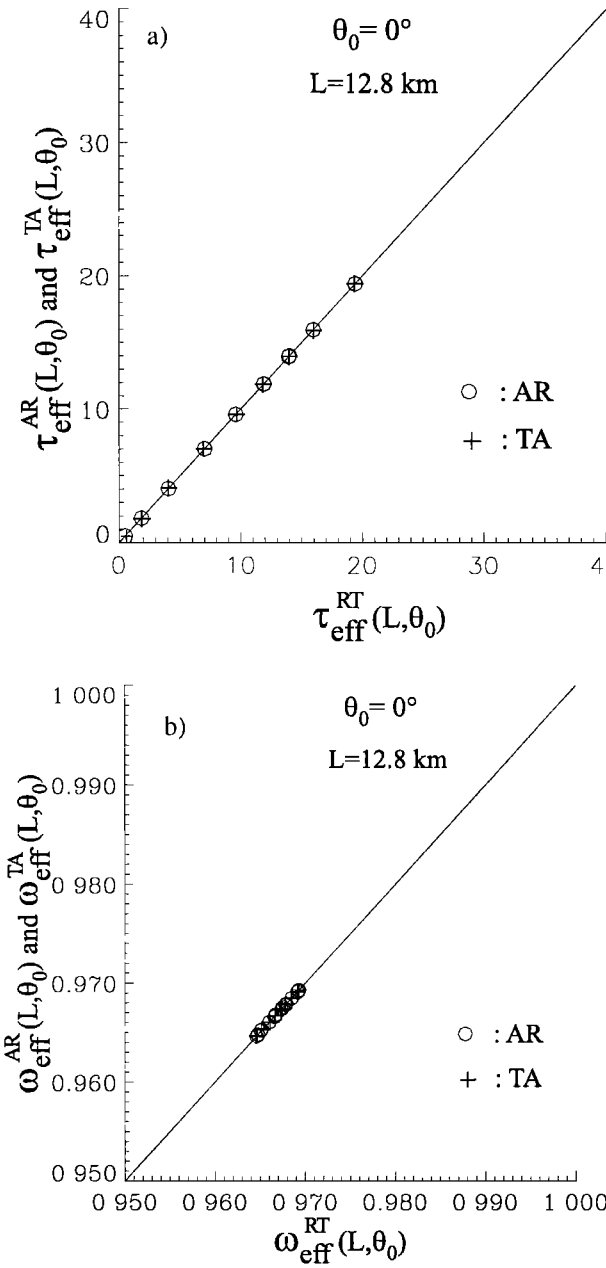

Figure 3. Comparison between different estimates of the effective optical depth and effective single scattering albedo: (a) $\tau^{AR}_{\text{eff}}(L)$ and $\tau^{TA}_{\text{eff}}(L)$ against $\tau^{RT}_{\text{eff}}(L)$, and (b) $\omega^{AR}_{\text{eff}}(L)$ and $\omega^{TA}_{\text{eff}}(L)$ against $\omega^{RT}_{\text{eff}}(L)$. Horizontal averaging scale: $L = 12.8$ km; incidence angle: $\theta_0 = 0°$; parameters estimated from (A,R) pair (circles), and from (T,A) pair (pluses).

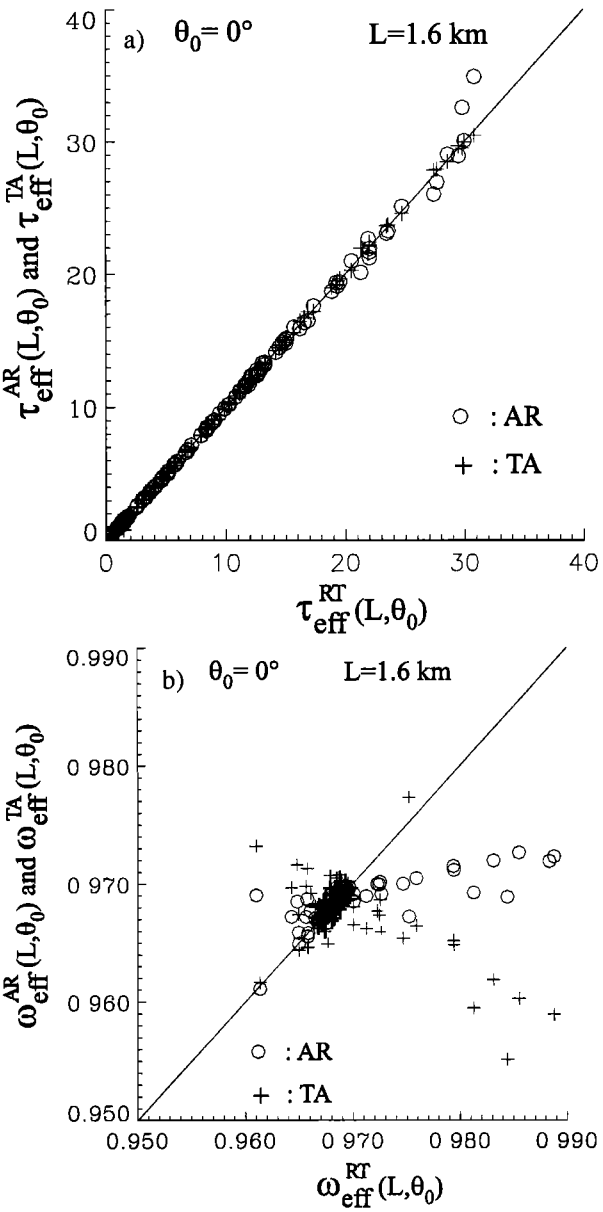

Figure 4. Same as Figure 3 but for $L = 1.6$ km.

of $\omega_{\text{eff}}(L)$ are located on or close to the bisector, except some points off the bisector. However, the number of "off-bisector" points remains small compared with the total number of points.

Figures 5 a and 5 b are the same as Figures 4 a and 4 b, but for $\theta_0 = 30°$. They exhibit the same general features as in Figures 4 a and 4 b except that the dispersion becomes significantly larger for $\theta_0 = 30°$ than $\theta_0 = 0°$. The correlation between different $\delta\omega_\varepsilon$ also becomes more evident in Figure 5 b than in Figure 4 b, because the ε term is more important in its magnitude for $\theta_0 = 30°$ than $\theta_0 = 0°$.

The deviations $\delta\tau_\varepsilon$ and $\delta\omega_\varepsilon$ depend on the partial derivatives of equation (3) and similar expressions. The partial derivatives $(\partial\tau^{RT}/\partial R)$, $(\partial\tau^{AR}/\partial R)$, and $(\partial\tau^{AR}/\partial A)$ are positive, while the others $(\partial\tau^{TA}/\partial A)$, $(\partial\tau^{TA}/\partial T)$, and $(\partial\tau^{RT}/\partial T)$ are negative. Hence $(\partial\tau^{RT}/\partial R)$ and $(\partial\tau^{RT}/\partial T)$ in $\delta\tau_\varepsilon(R,T)$ have the opposite signs and tend to compensate each other, while $(\partial\tau^{TA}/\partial T)$ and $(\partial\tau^{TA}/\partial A)$ in $\delta\tau_\varepsilon(T,A)$ $[(\partial\tau^{AR}/\partial A)$ and $(\partial\tau^{AR}/\partial R)$ in $\delta\tau_\varepsilon(A,R)]$ have the same sign and tend to reinforce each other.

As for the single scattering albedo, the partial derivatives $(\partial\omega^{RT}/\partial R)$, $(\partial\omega^{RT}/\partial T)$ and, $(\partial\omega^{AR}/\partial R)$ are positive, while the others $(\partial\omega^{TA}/\partial A)$, $(\partial\omega^{AR}/\partial A)$, and $(\partial\omega^{TA}/\partial T)$ are negative. Hence $(\partial\omega^{RT}/\partial R)$ and $(\partial\omega^{RT}/\partial T)$ in $\delta\omega_\varepsilon(R,T)$ $[(\partial\omega^{TA}/\partial A)$ and $(\partial\omega^{TA}/\partial T)$ in $\delta\omega_\varepsilon(T,A)]$ tend to reinforce each other, while $(\partial\omega^{AR}/\partial A)$ and $(\partial\omega^{AR}/\partial R)$ in $\delta\omega_\varepsilon(A,R)$ have the opposite signs and tend to compensate each other in most of the conditions. Hence $\delta\omega_\varepsilon(T,A)$ and $\delta\omega_\varepsilon(R,T)$ are

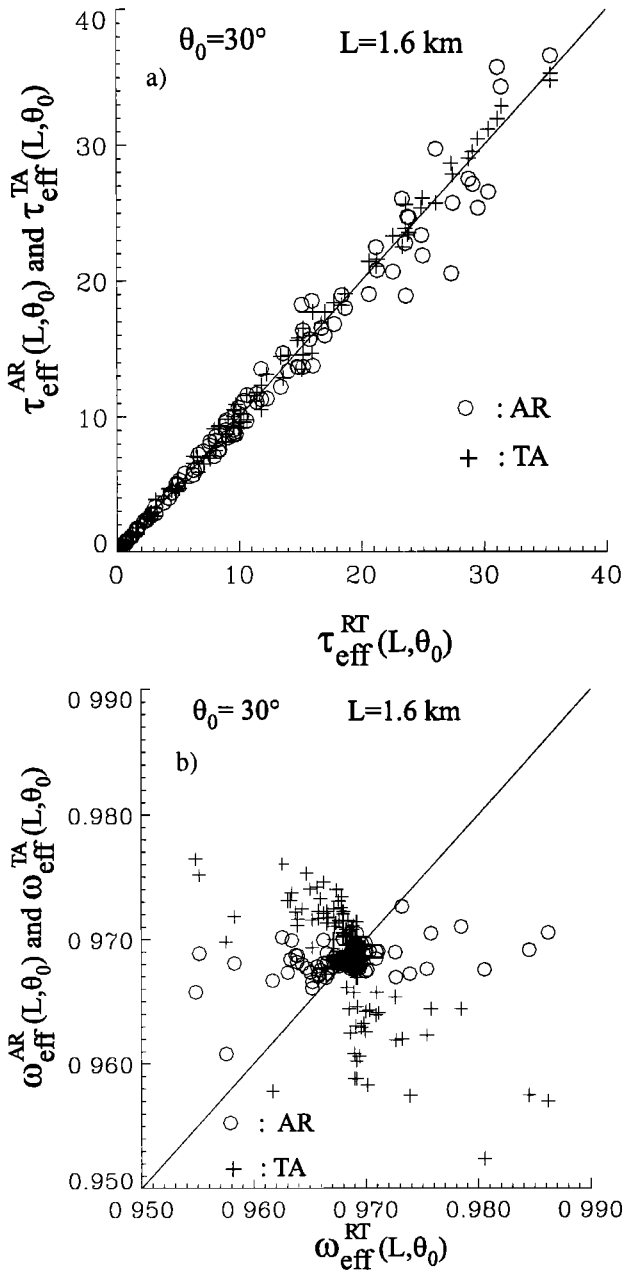

Figure 5. Same as Figure 4 but for $\theta_0 = 30°$.

of the opposite signs, and tend to be negatively correlated, while $\delta\omega_\varepsilon(A,R)$ and $\delta\omega_\varepsilon(R,T)$ tend to keep a weak positive correlation, as observed in Figure 4 b or Figure 5 b.

Any deviation from the bisector $\delta\tau_\varepsilon$ and $\delta\omega_\varepsilon$ results from the ε term effect, while the deviations $\delta\tau_{\text{int}}$ and $\delta\omega_{\text{int}}$ occur along the bisector. When the ε term is not nil, the three estimates of $\delta\tau_\varepsilon$ and $\delta\omega_\varepsilon$ are dependent (Equation (4)). Consequently, the effective radiative properties should exhibit different systematic bias, depending on which pair of radiant flux components is used to determine them. If $(R'_{\text{inhom}}, T'_{\text{inhom}}, A'_{\text{inhom}})$ were directly measured, the use of (R,T) pair would be the best to estimate $\tau_{\text{eff}}(L)$, and the use of (A,R) pair for $\omega_{\text{eff}}(L)$ because of the compensation effect.

We estimated the root-mean-square relative dispersion

$$D_{\text{disp}}\left(p_{\text{eff}}^{RT}, p_{\text{eff}}^{AR}\right) = \left\{ \frac{1}{2N} \sum_{i=1}^{N} \frac{\left[p_{\text{eff}}^{AR}(i) - p_{\text{eff}}^{RT}(i)\right]^2}{\left[p_{\text{eff}}^{AR}(i) + p_{\text{eff}}^{RT}(i)\right]^2} \right\}^{1/2} \tag{5}$$

for different averaging scales and incidence angles. N represents the number of data, and p_{eff} designates either τ_{eff} or ω_{eff}. We used only the data corresponding to $1.5 \leq \tau_{\text{eff}} \leq 60$ to estimate the relative dispersion because of a large dispersion observed for very small optical depths. Table 1 and Table 2 represent $D_{\text{disp}}(p_{\text{eff}}^{RT}, p_{\text{eff}}^{AR})$ for three incidence angles; the root-mean-square relative dispersions for other pairs are not shown, but they do not differ very much from those of Tables 1 and 2.

The small relative dispersions obtained for 12.8 km averaging confirm the "uniqueness" of both $\tau_{\text{eff}}(L)$ and $\omega_{\text{eff}}(L)$ at this scale of averaging. The relative dispersion increases as the horizontal averaging scale decreases from 12.8 km to 0.8 km but also as the solar incidence angle increases. D_{disp} of $\tau_{\text{eff}}(L)$ appears slightly smaller for the absorbing clouds than nonabsorbing clouds studied in SZl. The relative dispersion of $\omega_{\text{eff}}(L)$ also increases as the horizontal scale of averaging decreases from 12.8 km to 0.8 km. As seen in Figure 3 b the total range of variation of ω_{eff} is always about 0.5% of the nominal single-scattering albedo. D_{disp} of $\omega_{\text{eff}}(L)$ for the 3.2 km averaging is small in comparison with the total range of variation of $\omega_{\text{eff}}(L)$, while it becomes of the same order for the 1.6 km averaging. This means that we have to take an average over a horizontal scale much larger than the 1.6 km averaging to eliminate the ε effect on the effective single-scattering albedo.

Table 1. Relative Dispersion Between $\tau_{\text{eff}}^{AR}(L)$ and $\tau_{\text{eff}}^{RT}(L)$ as a Function of the Averaging Scale for $\theta_0 = 0°, 30°, 60°$

	D_{disp} Between τ_{eff}^{AR} and τ_{eff}^{RT}		
L, km	$\theta_0 = 0°$	$\theta_0 = 30°$	$\theta_0 = 60°$
12.8	7.4×10^{-5}	9.8×10^{-5}	7.9×10^{-5}
6.4	3.0×10^{-5}	1.2×10^{-5}	3.3×10^{-5}
3.2	1.0×10^{-2}	1.9×10^{-2}	5.5×10^{-2}
1.6	1.1×10^{-2}	4.2×10^{-2}	1.0×10^{-1}
0.8	3.6×10^{-2}	7.3×10^{-2}	1.7×10^{-1}

Only the data corresponding to $1.5 \leq \tau_{\text{eff}}$ are used to compute the relative dispersion.

Table 2. Relative Dispersion Between $\omega_{\text{eff}}^{AR}(L)$ and $\omega_{\text{eff}}^{RT}(L)$ as a Function of the Averaging Scale for $\theta_0 = 0°, 30°, 60°$

	D_{disp} between ω_{eff}^{AR} and ω_{eff}^{RT}		
L, km	$\theta_0 = 0°$	$\theta_0 = 30°$	$\theta_0 = 60°$
12.8	2.4×10^{-5}	2.8×10^{-5}	8.3×10^{-5}
6.4	2.1×10^{-5}	3.5×10^{-5}	7.8×10^{-5}
3.2	2.1×10^{-2}	3.5×10^{-2}	7.8×10^{-2}
1 6	2.5×10^{-2}	1.1×10^{-2}	2.4×10^{-1}
0.8	1.2×10^{-2}	2.3×10^{-2}	2.6×10^{-1}

Only the data corresponding to $1.5 \leq \tau_{\text{eff}}$ are used to compute the relative dispersion.

3.2.2. Dependency of $\tau_{\text{eff}}(L)$ and $\omega_{\text{eff}}(L)$ on the incidence angle. As discussed by SZ1, we need to examine the independence of $\tau_{\text{eff}}(L)$ and $\omega_{\text{eff}}(L)$ with respect to the solar incidence angle. This independence is desirable to define a completely equivalent PPH cloud. We made three series of special simulations for cloud-mean optical depths $\bar{\tau} = 0.5, 2, 5, 10, 15, 20, 25, 30,$ and 40, and for incidence angles of 0°, 30°, and 60° as in SZ1. We estimated $\tau_{\text{eff}}(L)$ and $\omega_{\text{eff}}(L)$ of each inhomogeneous cloud segment and computed the ratio of $\tau_{\text{eff}}(L)[\omega_{\text{eff}}(L)]$ between the 30° (60°) incidence and the 0° incidence angle

$$r_p(L, \theta_0) = \frac{p_{\text{eff}}(L, \theta_0)}{p_{\text{eff}}(L, 0°)}, \tag{6}$$

where $p_{\text{eff}}(L, \theta_0)$ designates the local effective parameter $p = \tau$ or ω estimated at the averaging scale L and for the solar incidence angle θ_0.

We estimated $r_p(L, \theta_0)$ for two averaging scales 12.8 km and 1.6 km. Figures 6 a and 6 b represent $r_\tau(L, 30°)$ and $r_\tau(L, 60°)$ for $\tau_{\text{eff}}^{RT}(L)$ and $r_\omega(L, 30°)$ and $r_\omega(L, 60°)$ for $\omega_{\text{eff}}^{RT}(L)$, respectively, as a function of $\bar{\tau}(L)$. In Figure 6 a, the ratios for the 12.8 km averaging are scattered around $r_\tau(L, \theta_0) = 1$. However, a close inspection reveals a systematic bias in $r_\tau(12.8 \text{ km}, 30°)$ and $r_\tau(12.8 \text{ km}, 60°)$ similar to those discussed in SZ1. In Figure 6 b a similar systematic bias exists but much smaller than the one observed for the effective optical depth (Table 3). For 1.6 km averaging, the dispersion of $\omega_{\text{eff}}(L)$ for $\theta_0 = 30°$ decreases rapidly from about 0.2% for $\tau_{\text{eff}} < 10$ to less than 0.1% for $20 < \tau_{\text{eff}}$; the dispersion for $\theta_0 = 60°$ is about twice the one for $\theta_0 = 30°$.

The above results indicate that we cannot define, "in stricto sensu", a unique PPH cloud, which has the same

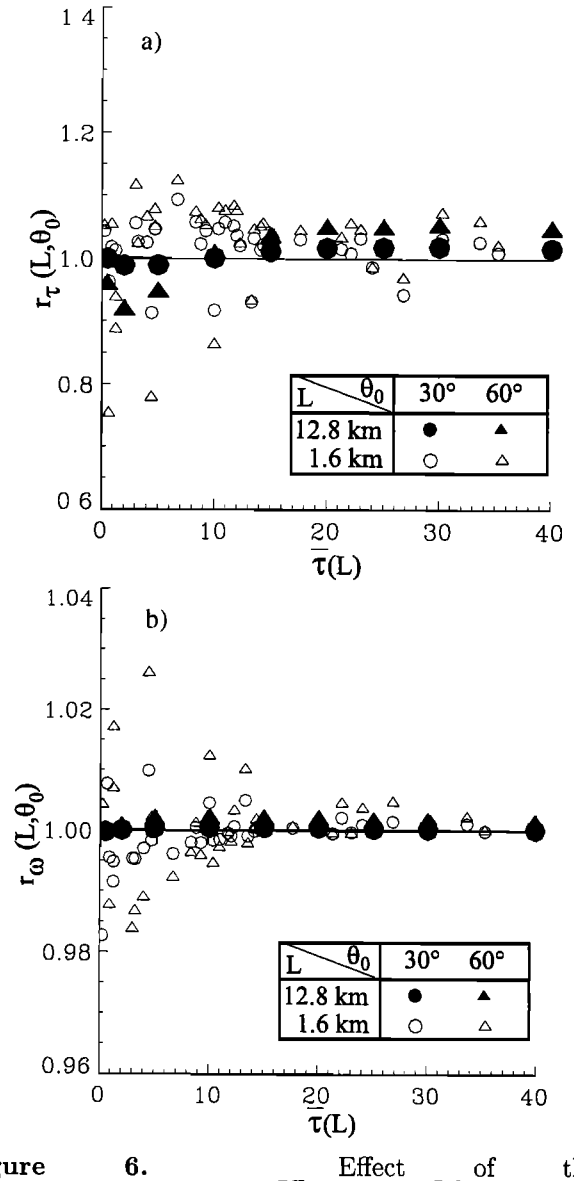

Figure 6. Effect of the incidence angle on $r_p = [p^{RT}_{eff}(L,30)]/[p^{RT}_{\text{eff}}(L,0°)]$ and $r_p = [p^{RT}_{\text{eff}}(L,60)]/[p^{RT}_{\text{eff}}(L,0°)]$ as a function of mean optical depth $\bar{\tau}(L)$ for two horizontal scales of averaging ($L = 12.8$ km and $L = 1.6$ km): (a) for $p = \tau$; (b) for $p = \omega$.

reflectance, transmittance and absorptance as those of an inhomogeneous absorbing cloud for any oblique illumination. This means that we can use a unique equivalent PPH cloud only if we admit some degree of error in the estimation of its radiant flux.

3.2.3. Error in the absorptance. From the practical point of view we often apply the PPH cloud assumption to an inhomogeneous cloud segment. For an inhomogeneous absorbing cloud we need two of the three fluxes ($R'_{\text{inhom}}, T'_{\text{inhom}}, A'_{\text{inhom}}$) to retrieve its effective radiative properties. R'_{inhom} and T'_{inhom} are often experimentally measured aboard aircraft. In this case we can retrieve $\tau^{RT}_{\text{eff}}(L)$ and $\omega^{RT}_{\text{eff}}(L)$ from these measurements and estimate the absorptance. We can show easily that the relative error in the absorptance is given by

$$\text{Error}\,[A(L,\theta_0)] \cong \frac{-\varepsilon}{A'_{\text{inhom}}(L,\theta_0)}. \tag{7}$$

For inhomogeneous absorbing clouds the absorptance increases at first rapidly and then more slowly with the mean optical depth, while the ε term also decreases rapidly after its initial increase with the mean optical depth. The relative error in the absorptance would be large for small optical depth, but it should decrease rapidly for large optical depth. This behavior of the relative error in the absorption differs significantly from that of the relative error in the transmittance of nonabsorbing clouds discussed by SZ1. Figures 7 a, 7 b, and 7 c show the relative error in the absorptance when $\tau^{RT}_{\text{eff}}(L)$ and $\omega^{RT}_{\text{eff}}(L)$ are retrieved from reflectance and transmittance averaged at horizontal scales of $L = 3.2$ km and $L = 1.6$ km. The relative error for 0° incidence and $L = 3.2$ km becomes less than about 5% for an optical depth larger than 5, while for 30° incidence, it becomes less than 5% only for an optical depth beyond 15. For 60° incidence, it remains larger than 5% for all optical depths less than 40. Accordingly, if we require a relative error in the absorptance less than 5%, we cannot use $\tau^{RT}_{\text{eff}}(L)$ and $\omega^{RT}_{\text{eff}}(L)$ retrieved at a horizontal scale of 3.2 km for an inhomogeneous cloud with 0.3 km in depth except for a cloud with a large optical depth under vertical illumination. This means that in processing aircraft measurement of radiant fluxes, we have to average them over a horizontal scale of averaging large enough to eliminate the ε effect on the absorptance.

3.3. Parametrization of $\tau_{\text{eff}}(L)$ and $\omega_{\text{eff}}(L)$

Empirical formulas are established for both $\tau^{RT}_{\text{eff}}L)$ and $\omega^{RT}_{\text{eff}}(L)$ as a function of the local mean optical depth and local cloud inhomogeneity. For this analysis we used all $\tau^{RT}_{\text{eff}}(L)$ $[\omega^{RT}_{\text{eff}}(L)]$ estimated at the averaging scales larger than 1.6 km [3.2 km for $\omega^{RT}_{\text{eff}}(L)$] and for the three incidence angles ($\theta_0 = 0°$, 30°, and 60°), although this would increases the dispersion.

We adjusted these data to an empirical relation:

$$\tau^{\text{cal}}_{\text{eff}} = \left\langle A\frac{1+B\bar{\tau}}{1+C\bar{\tau}}[1-\exp(D\rho_\tau)] + \bar{\tau}\{1+E[1-\exp(F\rho_\tau)]\}\right\rangle \cdot \left\langle 1-\exp\left\{-\frac{\bar{\tau}}{A[1-\exp(D\rho_\tau)]}\right\}\right\rangle, \tag{8}$$

where $\bar{\tau}$ and ρ_τ are the local mean optical depth and relative cloud inhomogeneity parameter estimated at the

Table 3. Variation of $R_\omega(12.8\text{ km},\theta_0) = [\omega_{\text{eff}}(12.8km,\theta_0)]/[\omega_{\text{eff}}(12.8\text{ km},0°)]$ Estimated for Two Incidence Angles ($\theta_0 = 30°$ and 60°) As a Function of the Mean Optical Depth $\bar{\tau}$

	$\bar{\tau} = 0.5$	5.0	15	25
$\theta_0 = 0°$	0.9998	1.0004	1.0005	1.0003
$\theta_0 = 60°$	0.9989	1.0009	1.0009	1.0005

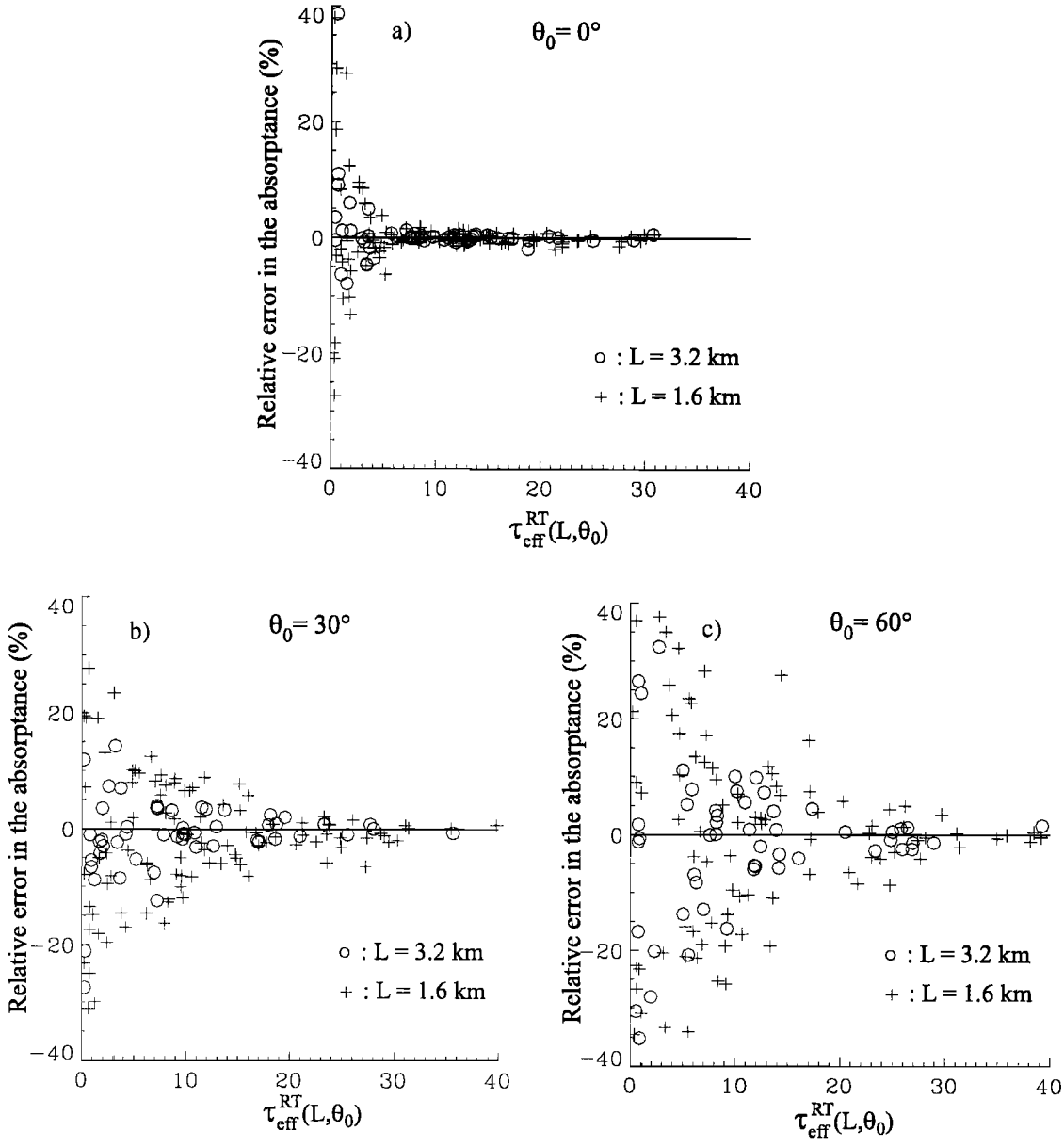

Figure 7. Effect of the incidence angle on the relative error in the absorptance when it is estimated from $\tau_{\text{eff}}^{RT}(L)$ and $\omega_{\text{eff}}^{RT}(L)$. Incidence angle: (a) $\theta_0 = 0°$; (b) $\theta_0 = 30°$; (c) $\theta_0 = 60°$. Horizontal averaging scale: circles, $L = 12.8$ km; pluses: $L = 1.6$ km.

averaging scale of L; we omitted the reference to L in equation (8). The constants are $A = -4.53 \times 10^{-3}$, $B = 1.57 \times 10^{-1}$, $C = 2.64 \times 10^{-1}$, $D = 8.17$, $E = 5.68 \times 10^{-2}$, and $F = 2.56$,respectively. To determine these constants, we adjusted only D and F for the absorbing cloud data, by keeping the other constants A, B, C, and E unchanged from those obtained for the non-absorbing clouds. For the nonabsorbing clouds we had $D = 12.6$ and $F = 3.78$.

Figure 8 compares $\tau_{\text{eff}}^{\text{cal}}(L)$ with $\tau_{\text{eff}}^{RT}(L)$. The $\tau_{\text{eff}}^{\text{cal}}(L)$ is computed with the local relative cloud inhomogeneity $\rho_\tau(L) = \sigma_\tau(L)/\bar{\tau}(L)$ in equation (8); $\sigma_\tau(L)$ and $\bar{\tau}(L)$ designate the local standard deviation of the optical depth and local mean optical depth, respectively. The dispersion around the bisector is quite similar to the one obtained for the nonabsorbing clouds in SZ1.

Figure 9 shows $\omega_{\text{eff}}^{RT}(L)$ estimated for the 12.8 km and 1.6 km averaging and for $\theta_0 = 0°$ as a function of $\bar{\tau}(L)$. $\omega_{\text{eff}}^{RT}(L)$ for 12.8 km averaging first decreases down to about 0.965 and then starts to increase but does not reach the nominal value. The dispersion is much larger for the 1.6 km averaging; some of $\omega_{\text{eff}}^{RT}(L)$ estimated for small $\bar{\tau}(L)$ become larger than the nominal value of 0.97, but most of them remain less than the nominal value for moderate to large $\bar{\tau}(L)$. We adjusted an empirical relation

$$\omega_{\text{eff}}^{\text{cal}} = \bar{\omega}\left[1 - A\rho_\tau^2 \bar{\tau}^\alpha \exp\left(-\frac{\bar{\tau}^\beta}{B}\right)\right] \tag{9}$$

with $\omega_{\text{eff}}^{RT}(L)$ obtained for all the averaging scales larger than 3.2 km (we did not include $\omega_{\text{eff}}^{RT}(L)$ obtained for

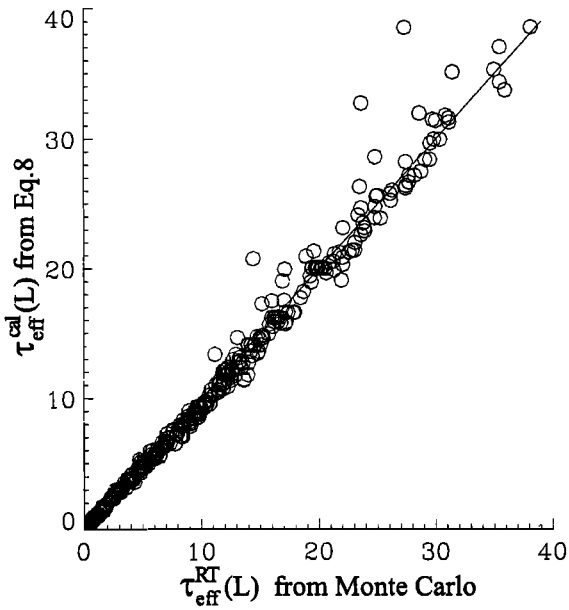

Figure 8. Comparison between $\tau_{\text{eff}}^{\text{cal}}(L)$ computed with equation (8) and $\tau_{\text{eff}}^{RT}(L)$ estimated directly from the area-averaged Monte Carlo reflectance and transmittance. The figure represents all $\tau_{\text{eff}}^{RT}(L)$ determined for $\theta_0 = 0°$, 30°, 60° and for all scales of averaging larger than 1.6 km.

the 1.6 km averaging). The constants are $A = 79.2$, $B = 9.65 \times 10^{-2}$, $\alpha = 3.29$, and $\beta = 0.214$, respectively.

Figure 10 compares $\omega_{\text{eff}}^{\text{cal}}$ with $\omega_{\text{eff}}^{RT}(L)$; $\omega_{\text{eff}}^{\text{cal}}$ were computed by using the local cloud inhomogeneity $\rho_\tau(L)$ in equation (9). We plotted only the points corresponding to $3 < \bar{\tau}(L)$, because of a larger dispersion for smaller mean optical depths. The dispersion around the bisector is moderate, and the data adjustment seems to be less satisfactory for ω_{eff}^{RT} than for $\tau_{\text{eff}}^{RT}(L)$.

As discussed by SZ1, the dispersion of Figure 8 and 10 results from three distinct causes: the choice of functions we chose to fit, the ε effect due to the nonzero net horizontal photon transport, and the uncertainty in the estimation of effective parameters. When the ε effect is negligible $[(\tau_{\text{eff}}^{RT} = \tau_{\text{eff}}^{TA} = \tau_{\text{eff}}^{AR})$ and $(\omega_{\text{eff}}^{RT} = \omega_{\text{eff}}^{TA} = \omega_{\text{eff}}^{AR})]$, we can fit, in principle, these data to other types of functions and improve the degree of approximation, if necessary, by including explicitly the incidence angle dependency of the effective optical depth and single-scattering albedo. As for the ε effect, we can minimize it under the EHCA, only by increasing the averaging scale. The use of $\bar{\tau}(L)$ and $\rho_\tau(L)$ in equations (8) and (9) assumes that the reflectance, transmittance, and absorptance of a cloud segment are completely conditioned by the optical and structural characteristics of the cloud segment. Such a condition is not always satisfied at a small averaging scale. The third possible cause is that the constant $\tau(R,T,A)$ and $\omega(R,T,A)$ curves of Figure 1 become too dense for small and large optical depths, and error in estimation of $\tau_{\text{eff}}(L)$ and $\omega_{\text{eff}}(L)$ may increase. Nevertheless, the above results show that the effective radiative properties of bounded cascade inhomogeneous clouds can be fairly well parameterized with the mean optical depth, single-scattering albedo, and relative cloud inhomogeneity, all of which are estimated at a given horizontal averaging scale.

4. Comparison Between EHCA and IPA

The difference between the EHCA and the IPA is conceptual, and it should depend on the importance

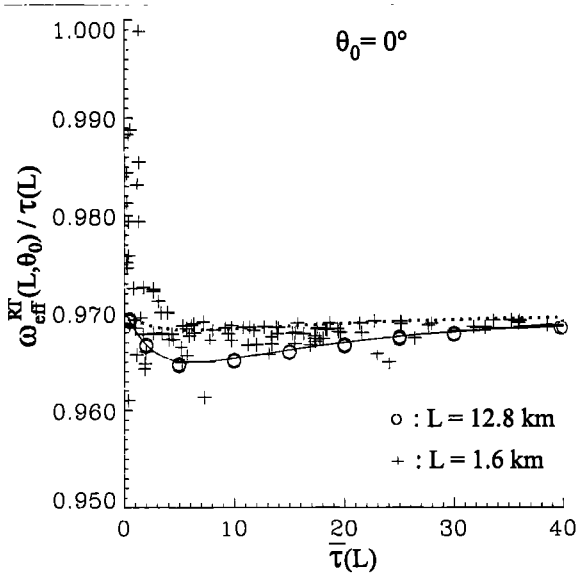

Figure 9. Variation of $\omega_{\text{eff}}^{RT}(L)$ as a function of the local mean optical depth $\bar{\tau}(L)$ for $\theta_0 = 0°$. Horizontal averaging scale: circles, $L = 12.8$ km; pluses: $L = 1.6$ km. Solid and dotted lines represent equation (9) with the mean relative cloud inhomogeneity estimated for the 12.8 km and 1.6 km averaging.

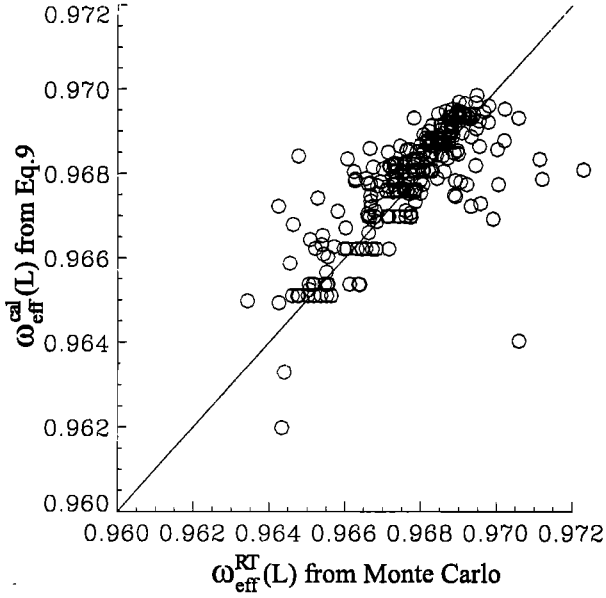

Figure 10. Comparison between $\omega_{\text{eff}}^{\text{cal}}(L)$ computed with equation (9) and $\omega_{\text{eff}}^{RT}(L)$ estimated directly from the area-averaged Monte Carlo reflectance and transmittance. The figure represents all $\omega_{\text{eff}}^{RT}(L)$ with $3 < \tau_{\text{eff}}$ determined for $\theta_0 = 0°$, 30°, 60°, and all scales of averaging larger than 3.2 km.

of the nonlinear effect of the radiative transfer: cloud inhomogeneity interaction (SZ1). The EHCA is based on the requirement of radiative flux and radiation budget equivalence on one hand, the definition of effective optical properties on the other. The IPA or NIPA basically are based on the smoothing effect of areaaveraging. Some of the discussions by SZ1 should still be valid for inhomogeneous absorbing clouds. Consequently, we will limit our discussion to what results from the inclusion of the absorption. We will examine first how the IPA works for the estimation of absorptance of inhomogeneous clouds. The second question, which is independent of the first question, is how the effective radiative properties of inhomogeneous absorbing clouds are to be defined within the framework of the ETA.

4.1. Application of EHCA and IPA to the Estimation of Absorptance

As noted by SZ1, both the IPA and the EHCA require "a priori" knowledge of cloud inhomogeneity to compute efficiently the area-averaged radiative flux of inhomogeneous absorbing clouds. No significant difference between nonabsorbing and absorbing clouds can be noticed in the estimation of the area-averaged reflectance and transmittance, when the averaging is done over a sufficiently large scale. Hence we will examine here only the performance of the IPA in the estimation of the absorptance.

Figure 11 represents the relative error in the absorptance between the MC and the IPA estimated for the 0°, 30°, and 60° incidences; the absorptance is estimated at the scale of the entire cloud domain, i.e., 12.8 km. For the 0° incidence the relative error is negative with a "maximum" of -5% for $0 < \bar{\tau} < 10$. It becomes positive for $10 < \bar{\tau}$ and stabilized at 2%. For the 30° incidence the transition point from negative to positive error moves to a smaller mean optical depth, and the relative error becomes positive beyond $\bar{\tau} \cong 2$ with a maximum error of about 3%. For the 60° incidence the relative error remains mainly positive, and after reaching a maximum of 5% at $\bar{\tau} \cong 5$, it steadily decreases to 3% beyond $\bar{\tau} \cong 5$. Contrary to the reflectance, the area-averaged IPA absorptance does not converge to a correct MC absorptance of the inhomogeneous absorbing clouds, which reveals the existence of the nonlinear effect of the radiative interaction, even if it is less than expected. This bias varies as a function of the cloud-mean optical depth and solar incidence angle.

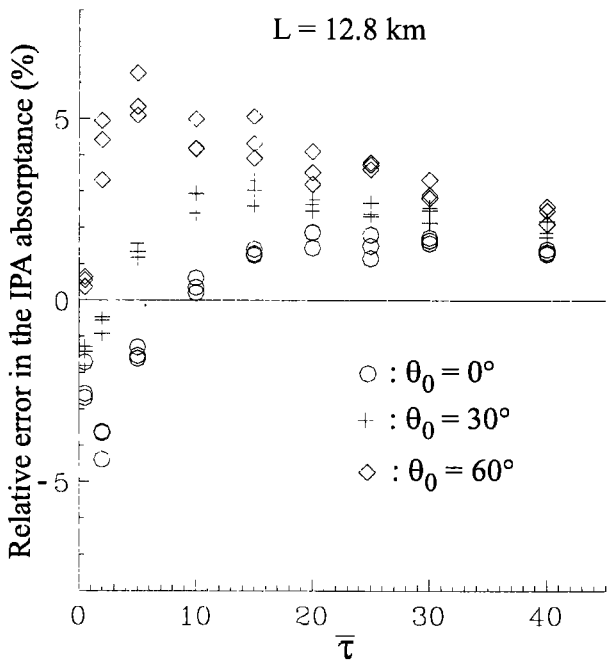

Figure 11. Relative error of the IPA absorptance $((A_{MC} - A_{IPA})/(A_{MC})\%)$ as a function of the cloud-mean optical depth $\bar{\tau}$. $L = 12.8$ km. Circles, $\theta_0 = 0°$; pluses, $\theta_0 = 30°$; diamond, $\theta_0 = 60°$.

4.2. Definition of τ_{eff} and ω_{eff} Within the EPA Framework

Cahalan et al. [1994a,b] introduced the ETA of an inhomogeneous nonabsorbing cloud, by taking the areaaverage of the Taylor expansion of the IPA cloud reflectance over the entire cloud domain. This effective optical depth is valid for only one cloud; for other clouds it is an approximation to τ_{eff} defined in the EHCA framework (SZ1). When we try to apply the same approach to an inhomogeneous absorbing cloud, we need to decide whether we are dealing with only the reflectance or with two of the three radiant flux components (reflectance, transmittance, and absorptance).

When only reflectance is considered, it would define an τ_{eff} similar to the one defined for the nonabsorbing clouds. In this case, the relation between τ_{eff} and $\bar{\tau}$ for the bounded cascade inhomogeneous absorbing clouds should be identical, by its principle, to that obtained for the nonabsorbing clouds ($\tau_{\text{eff}} = \tilde{\tau} = \beta\bar{\tau}$). However, the mean optical depth of the cloud, for which this relation is valid, should vary with the single-scattering albedo and solar incidence angle. The EHCA result shown above implies that the relation between τ_{eff} and $\bar{\tau}$ for the absorbing clouds should depend on the single-scattering albedo. Furthermore, this is exactly what *Borde and Isaka* [1996] did, which resulted in a systematic bias in the estimation of radiant flux components.

To define the effective single scattering in the ETA framework, we have to deal with two of the reflectance, transmittance, and absorptance. The area-averaged reflectance can be expressed approximately as

$$\overline{R(\ln\tau,\eta)} = R(\overline{\ln\tau},\bar{\eta}) + [\frac{\partial R}{\partial(\ln\tau)}]_{(\overline{\ln\tau},\bar{\eta})}\overline{\delta\ln\tau} + [\frac{\partial R}{\partial\eta}]_{(\overline{\ln\tau},\bar{\eta})}\overline{\delta\eta} + \frac{1}{2}[\frac{\partial^2 R}{\partial(\ln\tau)^2}]_{(\overline{\ln\tau},\bar{\eta})}\overline{(\delta\ln\tau)^2} + [\frac{\partial^2 R}{\partial(\ln\tau)\partial\eta}]_{(\overline{\ln\tau},\bar{\eta})}\overline{(\delta\ln\tau)\delta\eta} + \frac{1}{2}[\frac{\partial^2 R}{\partial\eta^2}]_{(\overline{\ln\tau},\bar{\eta})}\overline{(\delta\eta)^2} + \cdots \quad (10)$$

where η represents either $\ln\omega$ or ω. Values $\delta\eta$ and $\delta\ln\tau$ represent, respectively, the deviation from the corre-

sponding mean, i.e., $\eta - \bar{\eta}$ and $\ln\tau - \overline{\ln\tau}$. A similar expression can be written for the areaaveraged transmittance. For an inhomogeneous cloud with $\overline{\delta(\ln\tau)^2}$, $\overline{\delta\eta^2}$, $\overline{(\delta\ln\tau)\delta\eta} \neq 0$, the PPH cloud assumption $\overline{R(\ln\tau,\eta)} = R(\overline{\ln\tau},\bar{\eta})$ and $\overline{T(\ln\tau,\eta)} = T(\overline{\ln\tau},\bar{\eta})$ would be satisfied only for a cloud satisfying the following conditions:

$$[\frac{\partial^2 R}{\partial(\ln\tau)^2}]_{(\overline{\ln\tau},\bar{\eta})} = [\frac{\partial^2 R}{\partial(\ln\tau)\partial\eta}]_{(\overline{\ln\tau},\bar{\eta})} = [\frac{\partial^2 R}{\partial\eta^2}]_{(\overline{\ln\tau},\bar{\eta})} = [\frac{\partial^2 T}{\partial(\ln\tau)^2}]_{(\overline{\ln\tau},\bar{\eta})} = [\frac{\partial^2 T}{\partial(\ln\tau)\partial\eta}]_{(\overline{\ln\tau},\bar{\eta})} = [\frac{\partial^2 T}{\partial\eta^2}]_{(\overline{\ln\tau},\bar{\eta})} = 0. \quad (11)$$

If such a cloud with $(\overline{\ln\tau},\bar{\eta})$ is found (which is not guaranteed), τ_{eff} and ω_{eff} of an inhomogeneous absorbing cloud could be defined under the ETA; it would be possible, then, to extend the ETA to the "effective single-scattering albedo approximation". The exact expression of ω_{eff} depends on what type of spatial fluctuation is assumed for ω. For a special case with constant ω (constant η) the expressions $\overline{R(\ln\tau,\eta)} = R(\overline{\ln\tau},\bar{\eta})$ and $\overline{T(\ln\tau,\eta)} = T(\overline{\ln\tau},\bar{\eta})$ are valid only for an optical depth and single-scattering albedo satisfying $[\frac{\partial^2 R}{\partial(\ln\tau)^2}]_{(\overline{\ln\tau},\bar{\eta})} = [\frac{\partial^2 T}{\partial(\ln\tau)^2}]_{(\overline{\ln\tau},\bar{\eta})} = 0$. Accordingly, it is not possible to express $\bar{\eta}$ as a function of $\overline{\ln\tau}$ as we did in equation (9). This suggests that the effective single-scattering albedo cannot be properly defined within the ETA framework, because it is based on the IPA for which the notion of effective parameters is not intrinsic as it is for the EHCA.

5. Effective Single-Scattering Albedo and Anomalous Absorption Phenomenon

Since the recent publication of papers by *Cess et al.* [1995], *Ramanathan et al.* [1995], and *Pilewskie and Valero* [1995], there is a renewed interest in the anomalous absorption phenomenon [*Hayasaka et al.*, 1995; *Marshak et al.*, 1997, 1998]. Recently, *Titov* [1998] suggested that cloud inhomogeneity might contribute to the anomalous absorption phenomenon. The objective of this section is not to add one more paper to the already extensive anomalous absorption literature [*Stephens and Tsay*, 1990]. Its objective is rather to examine the implication of the EHCA with respect to the anomalous absorption phenomenon.

We have shown that the radiant flux should be averaged over a horizontal scale large enough to make the net horizontal photon transport negligible. For a one-dimensional (1-D) inhomogeneous cloud, a cloud aspect ratio of at least 20 is needed for the 60° incidence. When we compute the radiant flux components of observed natural clouds under the PPH cloud assumption, an important question arises: what optical depth and single-scattering albedo we have to use. According to the results presented in the previous sections, we have to use, in principle, τ_{eff} and ω_{eff} retrieved from measured area-averaged reflectance and transmittance to compute the radiant flux components under the PPH cloud assumption.

Let point C in Figure 12 (reproduced from Figure 2) be the measured reflectance and transmittance of an inhomogeneous cloud. The value of τ_{eff} can vary according to the way we estimate it, but also the information we estimate it from. Let us estimate τ_{eff} from either the measured reflectance or the transmittance on the $\omega(R,T,A) = 0.97$ curve by keeping the single-scattering albedo unchanged. When the reflectance (0.24) is used, we obtain τ_{eff} of about 5.8 (C'), which corresponds to a transmittance of 0.50. When the transmittance (0.42) is used, we obtain τ_{eff} of about 7.4, which gives a corresponding reflectance of 0.27 (C''). These reflectances and transmittances provide the absorptance of respectively 0.26 or 0.31, respectively, instead of the true value of 0.34. For the nearest points (average of the points C' and C'') the reflectance is 0.26 and transmittance 0.45, which results in an absorptance of about 0.29. According to these examples the absorptance of the inhomogeneous cloud estimated under the PPH cloud assumption becomes apparently smaller than the true absorptance of the inhomogeneous cloud by 10 to 25%. In other words, an inhomogeneous absorbing cloud behaves as if it has a larger value of the absorptance than that of an "equivalent" PPH cloud characterized by an effective optical depth and nominal single-scattering albedo.

It is to be emphasized that this enhanced absorption phenomenon is fictitious and results only from the assumption of constant single-scattering albedo under which we estimate τ_{eff} of the inhomogeneous cloud from either the reflectance or transmittance or both. Consequently, when we estimate the absorption of an inhomogeneous absorbing cloud in the framework of an equivalent PPH cloud, it is essential to take account of an apparent effect of cloud inhomogeneity on the single-scattering albedo and use an effective single-scattering albedo jointly with an effective optical depth. Doing otherwise may always lead to an apparent anomalous absorption phenomenon.

6. Conclusion

In this paper we investigated the effective radiative properties of inhomogeneous absorbing clouds generated with a bounded cascade process and compared their characteristics with those obtained for inhomogeneous nonabsorbing clouds. The major difference between the absorbing and nonabsorbing clouds resides in the fact that for an absorbing cloud we must define an effective single-scattering albedo in addition to an effective optical depth to treat the inhomogeneous clouds under the plane-parallel homogeneous cloud assumption. This finding implies that when the effective radius of inhomogeneous clouds is retrieved under the plane-parallel homogeneous cloud assumption, it would be slightly larger than the real mean effective radius.

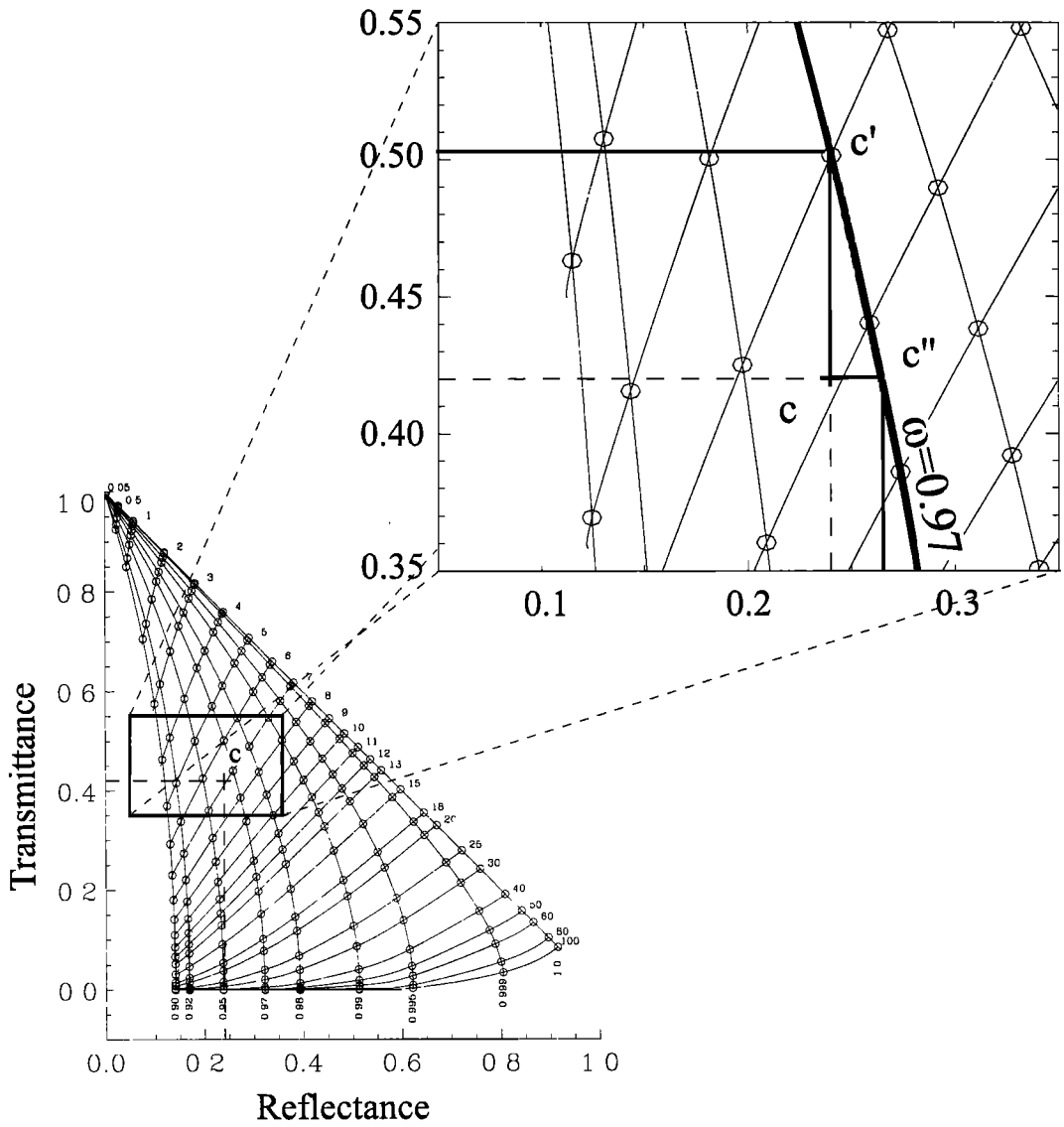

Figure 12. Schematic representation of various methods to estimate the absorptance of an inhomogeneous cloud under the plane-parallel homogeneous cloud assumption. The absorptance varies according to the methods used to estimate the effective optical depth of the inhomogeneous cloud from the measured reflectance and transmittance (point C). Point C' is estimated from the reflectance with the nominal single-scattering albedo. Point C'' is estimated from the transmittance with the nominal single-scattering albedo.

The effective parameters can be estimated from each one of three possible pairs of the area-averaged radiant flux components. They should agree with each other when the area-average is taken over a horizontal scale of averaging for which the net horizontal photon transport between the cloud segment and adjacent cloud cells can be neglected. For a smaller horizontal scale of averaging, some degree of dispersion always persists between these three pairs because of the nonzero ε term. The dispersion between these pairs varies as a function of the horizontal scale of averaging and the incidence angle of radiation in a way quite similar to that observed for the inhomogeneous nonabsorbing clouds in SZ1. These results suggest that the plane-parallel cloud model can be applied only when the radiant flux components are averaged over a horizontal scale much larger than the geometrical cloud depth.

The effective parameters vary with the mean optical depth, but also with the horizontal scale of averaging and relative local cloud inhomogeneity of the inhomogeneous cloud. Empirical relations were proposed for both the effective optical depth and the single-scattering albedo as a function of the local mean optical depth and relative local cloud inhomogeneity. However, the EHCA assumes that the reflectance, transmittance, and absorptance of a cloud segment are completely determined by its optical and structural characteristics.

We found that it is not possible to introduce properly an effective single-scattering albedo within the ETA framework on the basis of the IPA. Accordingly, there

is a significant conceptual difference between the ETA and the EHCA, even if they provide sometimes a numerically similar performance in estimation of the radiant flux of the bounded cascade inhomogeneous clouds.

When inhomogeneous clouds are generated with other processes, it is possible that most of the present results stand qualitatively without major modification but change quantitatively. We still need to investigate how the effective radiative properties of an inhomogeneous medium change with different types of inhomogeneity. In general, $\tau_{\text{eff}}(L)$ and $\omega_{\text{eff}}(L)$ should depend on the local mean optical depth $\bar{\tau}(L)$, inhomogeneity parameter of the optical depth $\rho_\tau(L)$, horizontal distance of averaging L, solar incidence angle θ_0, and also on other parameters. For example, they should depend eventually on the local mean single scattering albedo $\bar{\omega}(L)$ and the inhomogeneity parameter of the single-scattering albedo $\rho_\omega(L)$, if the single scattering albedo exhibits spatial variations. This means we need a more general approach to generate a stochastically inhomogeneous cloud and cloud field with statistical characteristics of natural clouds.

We finally discussed a possible implication of the effective single-scattering albedo, defined in this study, with respect to the anomalous absorption phenomenon. Not taking account of the apparent effect of cloud inhomogeneity on the single-scattering albedo may induce an apparent underestimation of the absorption, when an inhomogeneous absorbing cloud is treated in the framework of the equivalent plane-parallel homogeneous absorbing cloud.

Acknowledgments. This investigation was supported by the Japanese Space Agency (NASDA) grant, GLI/ADEOS II project G-0033, and French National Institute for Sciences of the Universe (INSU) grant, 96/ATP/494/220.2.

References

Borde, R., and H. Isaka, Radiative transfer in multifractal clouds, *J. Geophys. Res.*, *101*, 29,461-29,478, 1996.

Cahalan, R. F., W. Ridgway, W. J. Wiscombe, T. L. Bell, and J. B. Snider, The albedo of fractal stratocumulus clouds, *J. Atmos. Sci.*, *51*, 2434-2455, 1994a.

Cahalan, R. F., W. Ridgway, W. J. Wiscombe, S. Gollmer and Harshvardhan, Independent pixel and Monte Carlo estimates of stratocumulus albedo, *J. Atmos. Sci.*, *51*, 3776-3790, 1994b.

Cairns B., A. A. Lacis, and B. E. Carlson, Absorption within inhomogeneous clouds and its parameterization in general circulation models, *J.Atmos. Sci.*, in press, 2000.

Cess, R. D.,et al., Absorption of solar radiation by clouds: Observations versus models, *Science*, *267*, 496-499, 1995.

Davies, R., W. L. Ridgway, and K. E. Kim , Spectral absorption of solar radiation in cloudy atmospheres: A 20 cm^{-1} model, *J. Atmos. Sci.*, *41*, 2126-2137, 1984.

Davis, A. , A. Marshak, R. Cahalan, and W. Wiscombe, The Landsat scale break in stratocumulus as a three-dimensional radiative transfer effect: Implication for cloud remote sensing, *J. Atmos. Sci.*, *54*, 241-260, 1997.

Garcia, R., and C. Siewert, Benchmark results in radiative transfer, *Transp. Theory Statis. Phys.*, *14*, 437-484, 1985.

Hayasaka T., N Kikuchi, and M. Tanaka, Absorption of solar radiation by stratocumulus clouds: Aircraft measurement and theorical calculations, *J. Appl. Meteorol.*, *34*, 1047-1055, 1995.

Marshak, A., A. Davis, W. Wiscombe, and G Titov, The verisimilitude of the independent pixel approximation used in cloud remote sensing, *Remote Sens. Environ.*, *52*, 71-78, 1995.

Marshak, A., A. Davis, W. Wiscombe, and R. Cahalan, Inhomogeneity effects on cloud shortwave absorption measurements: Two-aircraft simulations, *J. Geophys. Res.*, *102*, 16,619-16,637, 1997.

Marshak, A., A. Davis, W. Wiscombe, W. Ridgway, and R. Cahalan, Biases in shortwave column absorption in the presence of fractal clouds, *J. Clim.*, *11*, 431-446, 1998.

Nakajima, T., and M. King, Cloud optical properties as derived from the multispectral cloud radiometer, paper presented at the FIRE Science Team Workshop. July 11-15, 1988.

Nakajima, T., and M. King, Determination of the optical thickness and effective particle radius of clouds from reflected solar measurements, Part I, Theory, *J. Atmos. Sci.*, *47*, 1878-1893, 1990.

Pilewskie P., and F. P. J. Valero, Direct observation of excess solar absorption by clouds, *Science*, *267*, 1626-1629, 1995.

Ramanathan, V., B. Subasilar, G. Zang, W. Connant, R. Cess, J. Kiehl, H. Grassl, and L. Shi, Warm pool budget and shortwave cloud forcing: A missing physics ?, *Science*, *267*, 499-503, 1995.

Stephens, G. L., and S. I. Tsay, On the cloud absorption anomaly, *Q. J. R Meteorol. Soc.*, *116*, 671-704, 1990.

Szczap, F., H. Isaka, M. Saute, B. Guillemet, and A. Ioltukhovski, Effective radiative properties of bounded cascade nonabsorbing clouds: Definition of the equivalent homogeneous cloud approximation, *J. Geophys. Res.*, this issue.

Titov G. A., Radiative horizontal transport and absorption in stratocumulus clouds, *J. Atmos. Sci.*, *55*, 2549-2560, 1998.

Twomey, S., and T. Cocks, Remotely sensing of cloud parameters from spectral reflectance in the near-infrared, *Contrib. Atmos. Phys.*, *62*, 172-179,1989.

Wetzel, M. A., and T. H. Vonder Haar, Theoretical development and sensitivity tests of stratus cloud droplet size retrieval method for AVHRR-K/UM, *Remote Sens. Environ.*, *36*, 105-109, 1991.

B. Guillemet, H. Isaka, M. Saute, F. Szczap, Laboratoire de Météorologie Physique, Université Blaise Pascal, 24 Avenue des Landais, 63177 Aubière Cedex, France.(e-mail:szczap@opgc.univ-bpclermont.fr)

A. Ioltukhovski, Keldish Institute of Applied Mathematics, 4 Miusskaya Pl. 125047 Moscow, Russia.

(Received March 19, 1999; revised November 8, 1999; accepted January 21, 2000.)